Competition between ices Ih and Ic in homogeneous water freezing

Alberto Zaragoza, Maria M. Conde, Jorge R. Espinosa, Chantal Valeriani, Carlos Vega, and Eduardo Sanz

Citation: The Journal of Chemical Physics **143**, 134504 (2015); doi: 10.1063/1.4931987
View online: http://dx.doi.org/10.1063/1.4931987
View Table of Contents: http://scitation.aip.org/content/aip/journal/jcp/143/13?ver=pdfcov
Published by the AIP Publishing

Competition between ices Ih and Ic in homogeneous water freezing

Alberto Zaragoza,[1] Maria M. Conde,[1,2] Jorge R. Espinosa,[1] Chantal Valeriani,[1,3] Carlos Vega,[1] and Eduardo Sanz[1]
[1]*Departamento de Quimica Fisica I, Facultad de Ciencias Quimicas, Universidad Complutense de Madrid, 28040 Madrid, Spain*
[2]*Laboratoire des Fluides Complexes et leurs Réservoirs, UMR 5150, Université de Pau et des Pays de l'Adour, B. P. 1155, Pau-Cedex 64013, France*
[3]*Departamento de Fisica Aplicada I, Facultad de Ciencias Fisicas, Universidad Complutense de Madrid, 28040 Madrid, Spain*

(Received 10 July 2015; accepted 17 September 2015; published online 6 October 2015)

The role of cubic ice, ice Ic, in the nucleation of ice from supercooled water has been widely debated in the past decade. Computer simulations can provide insightful information about the mechanism of ice nucleation at a molecular scale. In this work, we use molecular dynamics to study the competition between ice Ic and hexagonal ice, ice Ih, in the process of ice nucleation. Using a seeding approach, in which classical nucleation theory is combined with simulations of ice clusters embedded in supercooled water, we estimate the nucleation rate of ice for a pathway in which the critical nucleus has an Ic structure. Comparing our results with those previously obtained for ice Ih [Sanz *et al.*, J. Am. Chem. Soc. **135**, 15008 (2013)], we conclude that within the accuracy of our calculations both nucleation pathways have the same rate for the studied water models (TIP4P/Ice and TIP4P/2005). We examine in detail the factors that contribute to the nucleation rate and find that the chemical potential difference with the fluid, the attachment rate of particles to the cluster, and the ice-water interfacial free energy are the same within the estimated margin of error for both ice polymorphs. Furthermore, we study the morphology of the ice clusters and conclude that they have a spherical shape. © *2015 AIP Publishing LLC.* [http://dx.doi.org/10.1063/1.4931987]

I. INTRODUCTION

Understanding and characterizing in detail the freezing transition from supercooled liquid water to ice has a great relevance. For instance, the formation of ice in clouds has a strong influence in their ability to reflect solar radiation and is therefore an important factor in climate change.[1–3] Water freezing is also a key process in the cryopreservation of cells and tissues.[4] Moreover, ice formation is relevant to microbiology,[5] food industry,[6,7] materials science,[8] geology,[9] and physics.[10–16]

Water freezing starts by the nucleation of an ice cluster in supercooled water. The nucleation process can be homogeneous, if the cluster emerges in the bulk water, or heterogeneous, if it grows aided by surfaces or impurities. In the conditions found in high clouds, the nucleation of ice is believed to be homogeneous, which is the main motivation for the investigation of homogeneous ice nucleation. Homogeneous nucleation requires the formation of an ice cluster of a certain critical size above which the cluster can grow.

One of the fundamental questions regarding homogeneous ice nucleation is the structure of the critical cluster in terms of size, shape, and crystalline structure. This information cannot be extracted experimentally because the cluster is small (~nm) and short lived (~ns). Computer simulations have access to these length and time scales, so they are a suitable tool for investigating homogeneous ice nucleation. In fact, in the last few years there have been a few simulation studies of ice nucleation,[15,17–30] although a consensus over important quantities for nucleation such as the free energy barrier height, the cluster size, or the nucleation rate has not been reached yet. Moreover, only some of these works deal with the crystalline structure of the ice nucleus.[15,23,25,26]

By means of computer simulations, we have recently studied homogeneous ice nucleation assuming that ice clusters are spherical and have ice Ih structure.[19,20] In this work we revisit the problem and assess the validity of these two assumptions.

Ice Ih[31] is the stable ice polymorph at atmospheric pressure. However, this does not necessarily imply that ice nucleates via a Ih nucleus. According to Ostwald's step rule,[32] the structure of the critical cluster is that with the lowest nucleation free energy barrier, which may or may not coincide with the most stable phase. When ice is formed at low temperatures, a polymorph different from ice Ih is often obtained. This polymorph has been interpreted as being cubic ice (ice Ic[33]) in the past,[34–39] although more recently it has been reinterpreted as a structure with mixed cubic/hexagonal stacking.[26,40–42] The growth of ice with stacking disorder has also been observed in molecular simulations.[42–44] It has even been suggested that already at the level of the critical nucleus ice is formed with stacking disorder.[15,25,41,45] Ices Ic and Ih are stacking polymorphs characterised by an ABCABC and an ABAB stacking of planes in the direction perpendicular to the basal plane, respectively. When the temperature increases at 1 bar, ice polymorphs containing cubic stacking transform into pure ice Ih, proving that ice Ih is indeed the stable phase at least at high temperature.[46–51] However, ice Ih is marginally more stable than ice Ic (the enthalpy difference ranges from 35 to 160 J/mol depending on the experimental conditions[46,52–55]).

The aim of our work is to investigate the competition between ice Ic and Ih in the process of ice nucleation. We use the same approach as in Refs. 19 and 20 to study ice nucleation via ice Ic nuclei and compare the results with our previous calculations for ice Ih nuclei.[19,20] We conclude that within the accuracy of our calculations, both polymorphs nucleate with clusters of the same size and at the same rate, which is consistent with the experimental observation of ice with mixed stacking.[26,40–42]

We use the seeding technique to study ice nucleation.[56] This approach consists of inserting an ice seed in supercooled water and then calculating the temperature at which the cluster is critical and the attachment rate of particles to the cluster at that temperature. Since the polymorphic structure of the inserted cluster is chosen *a priori*, this technique allows us to separately study ice nucleation via ice Ic and Ih clusters and to compare the nucleation rate of these two pathways. Other simulation studies of homogeneous ice nucleation report the formation of small ice nuclei with mixed cubic/hexagonal stacking,[15,25,26] consistent with our result that the nucleation rate is the same for both polymorphs. To obtain the nucleation rate, we combine our calculations of simulations of the critical cluster size and of the rate at which particles attach to it, with Classical Nucleation Theory (CNT). This requires an accurate determination of the chemical potential of both solid polymorphs, which we perform by means of the Einstein molecule method,[57] based on the Einstein crystal method.[58] We find that for the selected water models (TIP4P/2005[59] and TIP4P/Ice[60]), both cubic and hexagonal ice have the same chemical potential within the accuracy of our calculations. The ice-liquid interfacial free energy is also the same for both polymorphs within our error bar. This is consistent with the observation of patches of cubic and hexagonal ice in the ice-water interface at coexistence conditions.[61]

Regarding the ice nucleus shape, in the past we have assumed it to be spherical.[19,20] This is a reasonable assumption given that a sphere minimizes the contact area, and therefore the interfacial free energy, between liquid water and ice. However, one could also argue that the crystalline symmetry could affect the shape of the ice cluster. Thus, ice Ic clusters could be cubic rather than spherical. We consider this possibility and use cubic clusters as well as spherical ones in our seeding scheme. We conclude that a sphere is the shape with the lowest free energy for the formation of ice clusters.

II. WATER INTERACTION POTENTIALS

Computer simulations of water and ices may be useful to interpret experimental results.[62,63] The main limitation of computer simulations is that the potential model used to describe the interaction between water molecules is approximate. Most popular potential models are rigid and non-polarizable and consist of a Lennard-Jones (LJ) center and some partial charges. An interesting question is whether these simple potentials are able to describe the phase diagram of water. In the past decade, it has been shown that models such as SPC/E[64] or TIP5P[65] fail in describing the phase diagram of water, whereas TIP4P[66] models are better to predict the phase diagram, at least qualitatively.[67] A new version of the TIP4P model was proposed in 2005, namely, TIP4P/2005.[59] This potential provides a reasonably good global description of real water.[59,68] Although TIP4P/2005 is probably the rigid non-polarizable model that best describes properties of liquid water,[63] it fails in predicting the melting temperature, underestimating it by more than 20 K.[59] By contrast, the TIP4P/Ice model[60] has been tailored to closely reproduce the coexistence temperature between ice Ih and liquid water at normal pressure. In this work we use both TIP4P/2005 and TIP4P/Ice to study the competition between ice Ih and ice Ic in the nucleation of ice from supercooled water at normal pressure.

III. GENERAL APPROACH

To investigate the competition between cubic and hexagonal ice in the process of ice nucleation, we calculate the nucleation rate, J, for clusters of each type of polymorph. Nucleation will proceed through the pathway with the highest J. To obtain J we use the seeding technique,[56,69] which has been successfully used to estimate the nucleation rate of hydrate clathrates,[70,71] sodium chloride,[72] and to study for homogeneous ice nucleation via hexagonal ice clusters.[19,20]

In the seeding approach, J is estimated by using the following expression based on Transition State Theory and CNT:[73–77]

$$J = Z f^{+} \rho_f \exp(-\Delta G_c/(k_B T)), \tag{1}$$

where $Z = \sqrt{|\Delta\mu|/(6\pi k_B T N_c)}$ is the Zeldovich factor (N_c being the number of particles in the critical cluster at a given temperature T, $|\Delta\mu|$ the chemical potential difference between ice and liquid water, and k_B the Boltzmann constant), f^{+} is the attachment rate of particles to the critical cluster, ρ_f is the density of liquid water, and ΔG_c is the height of the nucleation free energy barrier. We calculate the latter using the expression provided by CNT: $\Delta G_c = (N_c/2)|\Delta\mu|$. Therefore, to evaluate J we need to obtain N_c, $|\Delta\mu|$, f^{+}, and ρ_f. ρ_f is trivially calculated as an ensemble average in an NpT simulation (its value is given in Table III). In Secs. IV–VII, we describe how we calculate all the other quantities.

IV. CALCULATION OF $|\Delta\mu|$

To obtain $|\Delta\mu|$, we need to calculate separately the chemical potential of the solid and the fluid. We first describe the calculation of the chemical potential for the ice polymorphs.

A. Chemical potential of ices Ic and Ih

We determine free energies from Monte Carlo runs using the Einstein molecule method,[57] which is a variant of the Einstein crystal method.[58] We refer the reader to our previous works for details on how to implement this methodology for water.[57,78,79] Ewald sums are used to deal with Coulombic interactions. Both the LJ and the real parts of the Coulombic interactions are truncated at 9 Å. Long range corrections to energy and pressure are included in the LJ part of the potential.[80,81] Free energy calculations are performed at 200 K and 1 bar in the NVT ensemble (using the average density

and shape of the simulation box obtained from NpT runs in anisotropic Parrinello-Rahman simulations[82,83]). Once the Helmholtz free energy, A, is determined, the Gibbs free energy is obtained by simply adding the pV term. Typically, we use 16 different values of λ when implementing the Gauss-Legendre integration method connecting the real crystal to the ideal Einstein crystal. The maximum value of λ in the Einstein molecule calculations was of 25 000 (in k_BT units for the orientational and k_BT/Å^2 for the translational coupling). In the past we have typically used 80 000 (200 000) MC cycles to determine ΔA_2 (ΔA_1) (ΔA_1 and ΔA_2 are defined in Ref. 78). However, since the free energy difference between ice Ih and ice Ic is expected to be quite small, much longer runs are needed. In fact in this work, runs of 500 000 (1 000 000) cycles are used to determine ΔA_2 (ΔA_1). With these long runs, the statistical uncertainty of the free energy is about 0.002 in NkT units. This uncertainty was estimated from the standard deviation of the free energy obtained for a certain proton configuration after performing several independent calculations. However, this is not the only contribution to the uncertainty. For small systems, different proton arrangements may have different free energies. We use five independent proton configurations to estimate the free energy of ices Ih and Ic. The algorithm of Buch *et al.*[84] is used to generate proton disordered configurations having zero (or almost zero) net dipole moment. Note from Fig. 1 that the residual internal energy of ices Ic and Ih is the same within our accuracy. In Fig. 2, we show that the density is slightly lower for ice Ic. Due to this small density difference the enthalpy of ice Ic is about 0.002 J/mol higher than that of ice Ih at 1 bar, a negligible difference compared to the 35-160 J/mol found in experiments and in quantum calculations.[46,52–55,85] The results for the calculation of the chemical potential for the TIP4P/2005 model are presented in Table I.

There are several interesting aspects to comment on this table. The first one is that different proton configurations have different free energies. The difference between the configuration with the lowest and highest free energy is about 0.003 k_BT for ice Ih and about 0.005 k_BT for ice Ic. Averaging over proton disorder, the standard deviation is

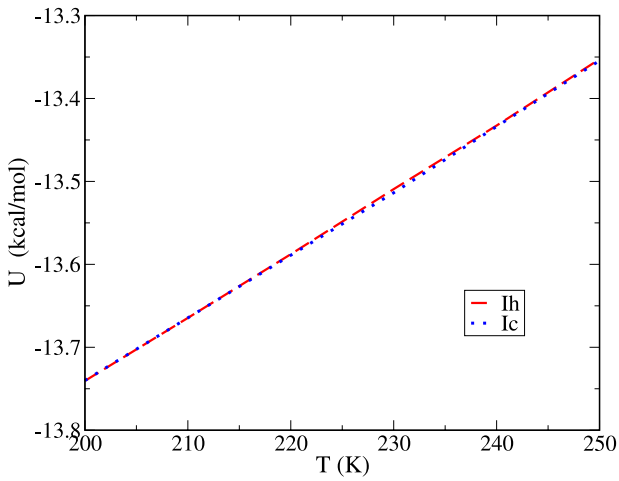

FIG. 1. Residual internal energy as a function of temperature for both ice polymorphs at 1 bar. The results correspond to the TIP4P/2005 model. The TIP4P/Ice model also gives indistinguishable internal energies for both ice structures.

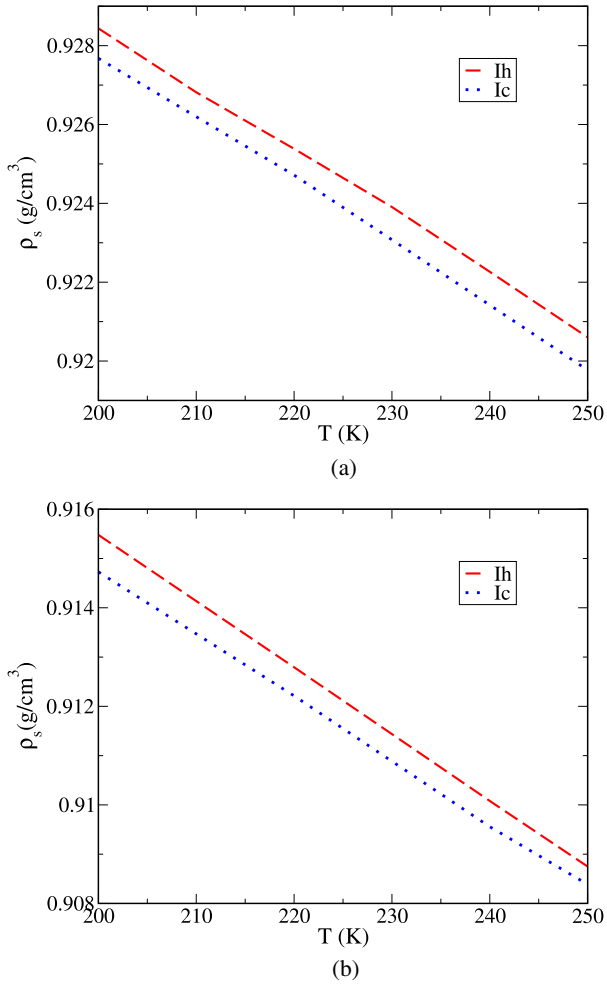

FIG. 2. Density versus temperature for ices Ih and Ic at 1 bar (see legend): (a) TIP4P/2005 model and (b) TIP4P/Ice model.

TABLE I. Free energy calculation for ices Ih and Ic at 200 K and 1 bar for the TIP4P/2005 model. The chemical potential μ (in k_BT units) is reported. The chemical potential is simply obtained as $\mu/(k_BT) = G/(Nk_BT) = A/(Nk_BT) + pV/(Nk_BT)$. Different proton arrangements were considered. The statistical uncertainty in the chemical potential for each proton disordered configuration is of about 0.002 k_BT. The standard deviation in chemical potential between different proton disordered configurations is of about 0.002 k_BT. Thus, the estimated error for the average free energy, reported in the last two lines, is of 0.004 k_BT. The de Broglie wavelength, Λ, has been set to 1 Å for these calculations.

Ice	Configuration	N	$\mu/(k_BT)$
Ih	1	432	−26.271(2)
Ih	2	432	−26.270(2)
Ih	3	432	−26.272(2)
Ih	4	432	−26.270(2)
Ih	5	432	−26.273(2)
Ic	1	512	−26.265(2)
Ic	2	512	−26.266(2)
Ic	3	512	−26.263(2)
Ic	4	512	−26.262(2)
Ic	5	512	−26.261(2)
Ih	Average	432	−26.271(4)
Ih	Average	512	−26.266(4)
Ic	Average	512	−26.264(4)

about 0.002 k_BT. Therefore, the total uncertainty of our free energy calculations is about 0.004 k_BT (0.002 from the error in determining the free energy of a certain proton disordered configuration and 0.002 from the standard deviation of the free energy between different proton disordered configurations). From this we can conclude that the free energy difference between the two ice polymorphs is rather small (and within the combined uncertainty of our calculations). Moreover, there is an additional factor that further reduces such difference. One should consider that free energy calculations of solids are affected by finite size effects. Usually the free energy increases with the system size. In fact for hard spheres it has been found that the free energy of the solid phase is smaller for small systems, and that the coexistence pressure of hard spheres increases with the system size (i.e., the stability of the solid phase is larger for small systems).[57,86,87] Even though the system sizes used here for ices Ih and Ic are quite similar (432 *vs.* 512), the number of particles is not exactly the same and this must be taken into account. For this purpose we performed free energy calculations of ice Ih for different system sizes (in particular we considered 288, 432, and 1024 particles) while keeping the cutoff constant at 8.5 Å. It was found that the free energy of ice Ih increases slightly with the system size (in agreement with the behavior found for hard spheres). The slope of G/NkT vs 1/N is of −13.8. To correct the free energy value obtained for ice Ih using 432 particles to a system size of 512, we simply use the expression −13.8 (1/512 − 1/432) = 0.005. In this way the estimated free energy of ice Ih for a system with 512 molecules is −26.271 + 0.005 = −26.266(4). Therefore, our estimate of the free energy of ice Ic with 512 particles is −26.264(4)NkT and that of ice Ih for a system of 512 particles is −26.266(4). Thus, we conclude that for the TIP4P/2005 model the free energy of ice Ih is slightly lower than that of ice Ic, but the difference is very small, and it is well within the error bar of the calculations.

Let us analyze if the similarity between the free energy of ices Ih and Ic extends to other TIP4P like models. In particular we consider the case of TIP4P and TIP4P/Ice. In previous work[59,60,88] we have shown that the phase diagram of these three TIP4P models is quite similar. In fact the main factor determining the aspect of the phase diagram of a water model is the way the partial charges are located within the molecule (as this affects significantly the value of the quadrupole moment[89]). For these models we do not undertake a study as extensive as for the TIP4P/2005 model and the estimated error of our calculations is now about 0.01 k_BT, 0.005 arising from the statistical uncertainty of the free energy calculations for a certain configuration and 0.005 from the fact that we use only one proton disordered configuration. The results for TIP4P and TIP4P/Ice are presented in Table III and confirm that both ice polymorphs have the same chemical potential also for these models.

B. $|\Delta\mu|$

As discussed in Sec. IV A, the chemical potential of both ice polymorphs is the same within accuracy for both TIP4P/2005 and TIP4P/Ice. Therefore, the chemical potential difference with respect to liquid water is also the same. Such difference is reported for both models in Ref. 20 (Fig. 2 and Table II), where we studied homogeneous ice nucleation via ice Ih clusters. The fact that both ice polymorphs have the same chemical potential also implies that they have the same melting temperature.

TABLE II. Chemical potential of ices Ih and Ic at 200 K and 1 bar as obtained from free energy calculations of the solid phase using the Einstein molecule method for the TIP4P and TIP4P/Ice models.

Model	Ice	N	$\mu/(kT)$
TIP4P/ICE	Ih	432	−29.53(1)
	Ic	512	−29.53(1)
TIP4P	Ih	432	−22.95(1)
	Ic	512	−22.95(1)

V. CALCULATION OF N_c

The results presented in the remainder of the paper have been obtained with NpT molecular dynamics simulations using the GROMACS package.[90] We refer the reader to our previous works dealing with ice Ih clusters for the simulation details.[19,20]

To obtain N_c via the seeding technique, a crystalline cluster is inserted in the supercooled fluid (the cluster is apolar and obtained from an orientationally disordered ice lattice using the algorithm of Ref. 84 imposing the dipolar moment equal to zero). Then, the interface between the cluster and the fluid is equilibrated by running a short simulation at low temperatures,[19,20] after which the cluster is left with N_c molecules. Finally, the number of particles in the cluster, N, is monitored for several MD simulations launched at different temperatures (in the Appendix we explain the way the number of particles in the cluster is identified). For temperatures higher than the one at which the cluster is critical, the cluster will melt, and vice versa. Therefore, the temperature at which the inserted cluster is critical is enclosed between the highest temperature at which it grows and the lowest at which it melts. In Fig. 3, we show the MD trajectories used to identify the temperature at which an ice Ic cluster of ∼3500 molecules

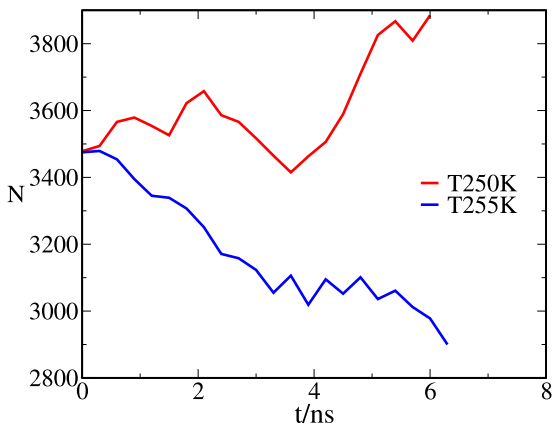

FIG. 3. Number of molecules in the cluster, N, as a function of time (ns) for an ice Ic cluster of $N_c = 3475$ molecules. The cluster is critical at a temperature between 250 K (red curve) and 255 K (blue curve). Results are for TIP4P/Ice at 1 bar.

TABLE III. Reported for a given cluster are the corresponding size, N_c, the total number of molecules (cluster plus surrounding liquid) in the simulation box, N_T, and the temperature at which the cluster is found to be critical, T_c/K. For that temperature we report the supercooling, ΔT/K, the fluid density, $\rho_f/(\mathrm{g/cm^3})$, the chemical potential difference between the liquid and the solid, $|\Delta\mu|$ (kcal/mol), the interfacial free energy, $\gamma/(\mathrm{mN/m})$, the height of the nucleation free energy barrier, $\Delta G_c/(\mathrm{k_B T})$, the Zeldovich factor, Z, the attachment rate, $f^+/\mathrm{s^{-1}}$, and the decimal logarithm of the nucleation rate, $\log_{10}(\mathrm{J/(m^{-3}\ s^{-1})})$. Results for ice Ic correspond to this work and those for ice Ih to previous work by some of the authors.[19,20]

Model	Ice	N_c	N_T	T_c	ΔT	ρ_f	$\lvert\Delta\mu\rvert$	γ	ΔG_c	Z	f^+	$\log_{10} J$
TIP4P/ICE	Ic	643	22 724	240.0	32.0	0.952	0.126	22.8	85	4.66×10^{-3}	1.20×10^{11}	2
TIP4P/ICE	Ic	3475	76 809	252.5	19.5	0.971	0.083	26.3	288	1.59×10^{-3}	3.24×10^{12}	−86
TIP4P/ICE	Ic	7934	182 663	257.5	14.5	0.975	0.063	26.40	489	9.07×10^{-4}	6.11×10^{12}	−174
TIP4P/ICE	Ih	600	22 712	237.5	34.5	0.952	0.133	23.7	85	5.00×10^{-3}	3.00×10^{11}	1
TIP4P/ICE	Ih	3167	76 781	252.5	19.5	0.971	0.083	25.40	261	1.66×10^{-3}	2.90×10^{12}	−75
TIP4P/ICE	Ih	7926	182 585	257.5	14.5	0.975	0.063	26.30	487	9.07×10^{-4}	6.90×10^{12}	−173
TIP4P/2005	Ic	3475	76 809	232.5	19.5	0.976	0.0801	25.6	308	1.61×10^{-3}	1.2×10^{12}	−96
TIP4P/2005	Ih	3170	76 781	232.5	19.5	0.976	0.0801	25.0	275	1.70×10^{-3}	1.2×10^{12}	−83

is critical for TIP4P/Ice. In view of the trajectories shown in Fig. 3, we conclude that the cluster is critical at a temperature of 252.5 ± 2.5 K. This temperature is the same as that found for an ice Ih cluster of a similar size.[19,20] We study cluster sizes from ∼10^3 to ∼10^4 water molecules. These calculations are computationally demanding because in order to avoid the cluster interacting with its periodic images we have to embed it in a liquid with approximately 20 times as many molecules as the cluster. To cope with simulations of such scale we resorted to parallel MD computations. We limited our study to three cluster sizes for TIP4P/Ice and one for TIP4P/2005. In Table III, we summarize our results for the temperature at which ice Ic clusters of different sizes are critical and compare them with those obtained in Refs. 19 and 20 for ice Ih clusters of similar sizes. Within the error of our calculation, ±2.5 K, similar size ice Ih and Ic clusters are critical at the same temperature. In Fig. 4, we plot the size of the critical cluster versus the supercooling (the temperature difference between the melting temperature and the temperature of interest) for both ice Ih and Ic clusters. The figure shows that for a given supercooling both ice polymorphs nucleate via clusters of the same size. Note also that both models predict critical clusters of the same size for the same supercooling. This is true for all studied models of the TIP4P family.[19,20]

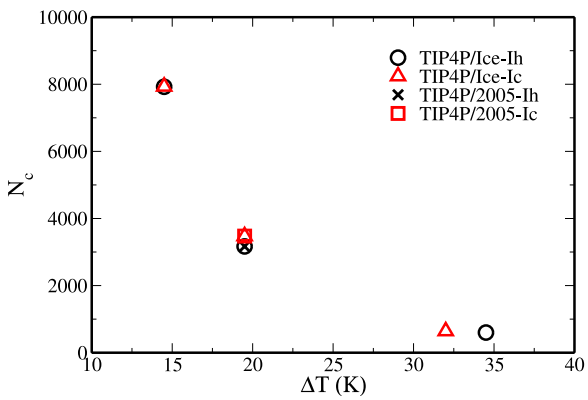

FIG. 4. Critical cluster size versus supercooling, ΔT, for both ice polymorphs and water models.

VI. CALCULATION OF f^+

To obtain the attachment rate f^+, we follow Refs. 76 and 77,

$$f^+ = \frac{\langle (N(t) - N_c)^2 \rangle}{2t}. \tag{2}$$

In the equation above, $N(t)$ is the number of particles in the cluster at time t and the average is obtained over ∼10 MD trajectories starting from a cluster of critical size and performed at the temperature at which the cluster is critical. All trajectories are started from the same configuration but with a different Maxwell-Boltzmann velocity distribution. The average of $(N(t) - N_c)^2$ is only calculated after 0.5 ns to avoid memory effects.[91] In Fig. 5, we show $N(t)$ for such simulations starting from an ice Ic cluster of ∼3500 particles. Note that in some trajectories the cluster grows, in others it shrinks, while in some others it neither grows nor shrinks. With the trajectories shown in Fig. 5, we obtain a plot of $\langle (N(t) - N_c)^2 \rangle$ versus time (Fig. 6) and evaluate f^+ from the slope. The slopes shown in Fig. 6 are very similar for both ice polymorphs, which means that the attachment rate of particles to the critical cluster does

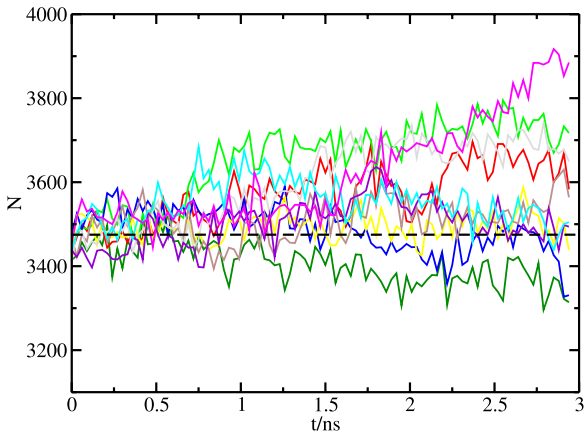

FIG. 5. Number of particles in the cluster versus time for different trajectories starting from an ice Ic critical cluster of 3475 water molecules. Runs correspond to the TIP4P/Ice model at T = 252.5 K, the temperature at which the cluster is critical at 1 bar.

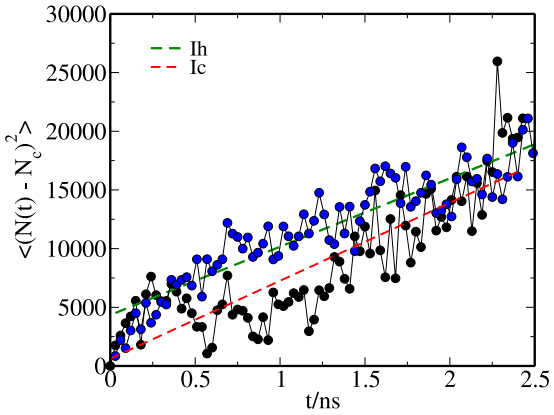

FIG. 6. $\langle (N(t)-N_c)^2 \rangle$ versus time for ice Ic (black circles) and Ih (blue circles) clusters with ~3500 particles at 252.5 K (TIP4P/Ice model). Dashed lines are linear fits to the data (the slope of such fits divided by 2 gives the attachment rate f^+).

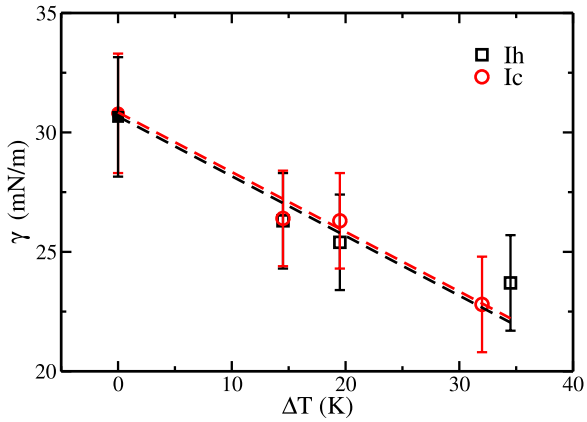

FIG. 7. Interfacial free energy for ice Ic (red empty circles) and ice Ih (black empty squares) as a function of the supercooling for the TIP4P/Ice model. Dashed lines are linear fits with slope −0.25 mN/(m·K)[20] to each set of data and full symbols correspond to the extrapolation of such fits to coexistence conditions ($\Delta T = 0$).

not change from hexagonal to cubic clusters. In Table III, we report the attachment rate of all ice Ic clusters studied in this work as well as that for ice Ih clusters previously obtained.[19,20]

VII. EVALUATION OF THE NUCLEATION RATE, *J*

Once N_c, $|\Delta\mu|$, f^+, and ρ_f are evaluated as described above, we can obtain J via Eq. (1). The fact that both ice polymorphs give, within the accuracy of our method, the same result for the aforementioned quantities already anticipates that the nucleation rate via ice Ih and Ic clusters will also be the same. This is shown in Fig. 8, where we plot with symbols our results of J for the ice Ic clusters studied in this work as a function of the supercooling and compare it with the results previously obtained for ice Ih clusters.[19,20] The values of J are also reported in Table III. The prediction of both water models employed is that ice nucleates at the same rate regardless whether nucleation proceeds via ice Ih or Ic nuclei.

A. Fits to the *J* data and *γ*

In order to estimate the rate for a wide temperature range, we use the same procedure as in Ref. 20 to obtain a curve that fits our J data. For TIP4P/Ice, to obtain such curve we first need to obtain the dependency of the crystal-fluid interfacial free energy, γ, with temperature. This can be done by estimating γ for each studied cluster size through the following CNT expression for spherical clusters:

$$\gamma = \frac{|\Delta\mu|}{2}\left(\frac{3N_c\rho_s^2}{4\pi}\right)^{1/3}. \quad (3)$$

The only new variable that is introduced in this expression with respect to those used for the calculation of J is ρ_s, the density of ice, that can be easily calculated via standard NpT simulations. In Fig. 2, we show ρ_s as a function of temperature for both polymorphs and for both models. ρ_s is the only thermodynamic variable for which we obtained a difference between both polymorphs. The difference, nevertheless, is very small (less than 0.01%) and it does not significantly affect the value of γ. In Fig. 7, we show γ versus supercooling for the ice Ic nuclei considered in this work and compare them with the values previously obtained for ice Ih (for the TIP4P/Ice model).[19,20] The ice Ic-liquid and ice Ih-liquid interfaces have the same interfacial free energy within the accuracy of our calculations. To obtain the dependency of γ with T, we fit the data in Fig. 7 to a straight line of slope −0.25 mN/(m·K), which is the average slope between different models of the TIP4P family.[20] The extrapolation of $\gamma(T)$ to $\Delta T = 0$ gives the interfacial free energy for the flat ice-water interface at coexistence conditions. The value obtained of 31 ± 3 mN/m is consistent with experimental data,[10,92] although this is not so difficult considering the wide range of published experimental values for the ice-water interfacial free energy.[10,92] Moreover, the value we get for γ is also consistent with that of other TIP4P models for which γ has been computed directly from numerical simulations at coexistence.[61,93]

Once $\gamma(T)$ is known we can obtain $\Delta G_c(T)$ as $16\pi\gamma^3/(3\rho_s^2|\Delta\mu|^2)$. With that, we can calculate the exponential factor in the expression for J given by Eq. (1). We only need to know the dependency of the attachment rate f^+ with temperature to obtain a $J(T)$ curve that can fit our data. To obtain such

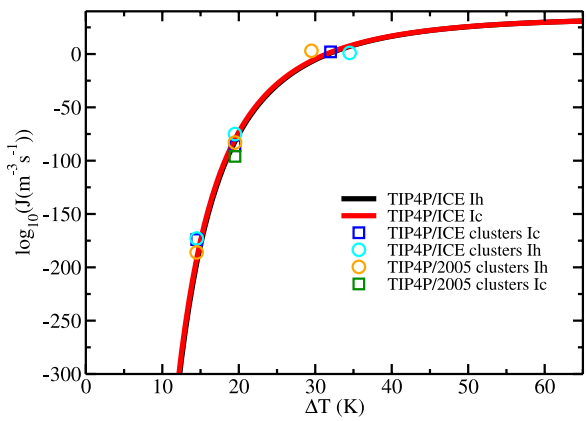

FIG. 8. Nucleation rate via ice Ic (this work) and Ih (Refs. 19 and 20) clusters as a function of supercooling. Symbols correspond to the calculation of J via Eq. (1) and solid lines to a CNT fit to our data obtained as discussed in the main text. (Table III).

dependency, we use the following CNT expression for the attachment rate: $f^+ = \frac{24D(N_c)^{2/3}}{\lambda^2}$, where D is the diffusion coefficient of the fluid and λ is the typical distance travelled by a particle to attach to the cluster. In Ref. 20, we give an expression for $D(T)$ and show that the CNT expression for f^+ fits well the attachment rate calculated by means of Eq. (2) for $\lambda = 5$ Å. Having computed $f^+(T)$ we combine it with the functions $\Delta\mu(T)$, $\rho_s(T)$, and $\Delta G_c(T)$ above discussed to draw a curve for $J(T)$ as shown in Fig. 8. As expected, the nucleation rate curves for cubic and hexagonal clusters are almost identical. They fit well with our data (by construction) and predict the nucleation rate for a wide range of supercooling.

VIII. STUDY OF THE CLUSTER SHAPE

The ice Ic clusters examined in this work and the ice Ih clusters investigated in Refs. 19 and 20 were inserted with a spherical shape. According to CNT, a sphere should be the preferred cluster shape given that it minimizes the contact surface between the solid and the liquid. However, this is an assumption that deserves being further investigated. One could also hypothesize that the shape of the unit cell is reflected in that of the critical nucleus. In such case, ice Ic nuclei should have a cubic rather than spherical shape. To study this hypothesis we inserted a cubic ice Ic cluster with ~4000 molecules in supercooled TIP4P/Ice water and followed its behaviour. The inserted cubic cluster exposes the (100), (010), and (001) planes to the fluid. As usual, we first equilibrated the interface for 0.2 ns at 200 K and then let the cluster evolve at 255 K, a temperature close to that at which a spherical cluster with a similar number of molecules is critical. The evolution of the cluster's shape is shown as a sequence of snapshots in Fig. 9, where it can be clearly seen that the cluster adopts a spherical shape in less than 2 ns. This means that it is the interfacial free energy, and not the symmetry of the unit cell, that determines the shape of ice nuclei. The same has been observed for NaCl nuclei,[72] although when clusters are small enough their shape can be influenced by that of the unit cell.[72,94]

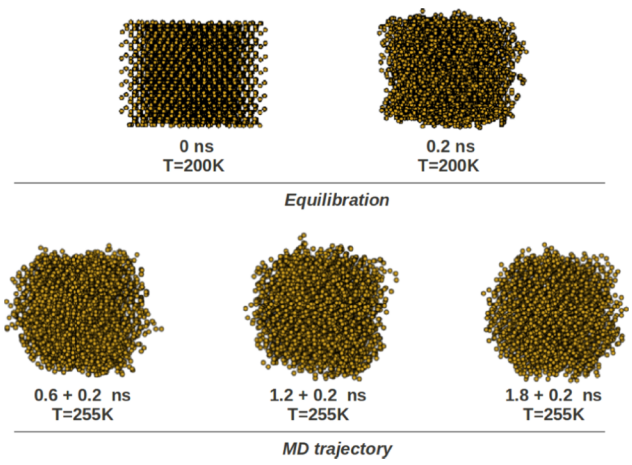

FIG. 9. Snapshots of the evolution of a cubic Ic cluster. In the top row, we represent the cubic cluster as initially inserted and after 0.2 ns equilibration time at 200 K. In the bottom row, we show subsequent snapshots of the cluster during an NpT simulation at 1 bar and 255 K. In less than 2 ns the cluster loses the cubical shape and becomes spherical.

IX. DISCUSSION

We now discuss the error of the main variables in Table III. The statistical uncertainty in ΔT is of about 2.5 K. This yields an error of about 7% in $\Delta\mu$, γ, and ΔG_c. Consequently, the absolute error in $\log_{10} J$ is that of ΔG_c divided by 2.3 (from the conversion of natural to decimal logarithm). As discussed in Refs. 19 and 20, the determination of N_c via a local order parameter might be subject to a systematic error that would add up to the statistical error. Within reasonable choices of the order parameter, such systematic error would be at most of the same order of the statistical one for ΔG_c and $\log J$, and about one third of the statistical error for γ.

By means of free energy calculations, we conclude that the chemical potential is the same for both ice Ih and Ic polymorphs for the following water models: TIP4P, TIP4P/2005, and TIP4P/Ice. Also for the ST2 model, Smallenburg and coworkers have recently shown that ices Ih and Ic have quite similar free energies.[95] Therefore, all these models predict that ice Ic and Ih are equally stable at normal pressure and have the same melting temperature. This clashes with the experimental fact that ice with cubic stacking formed at low temperatures transforms into pure ice Ih on heating.[46] For the mW model,[96] it has been reported that ice Ih is slightly more stable than ice Ic.[96,97] However, recent free energy calculations were not able to discriminate between both ice polymorphs.[98] In a recent publication, it has been argued that the greater stability of ice Ih is due to nuclear quantum effects,[85] which makes it very difficult for simple classical water models to quantitatively predict the relative stability of both ice I polymorphs.

The models employed in this work predict that the nucleation rate of ice is the same regardless the structure, Ih or Ic, via which ice starts growing. Therefore, one might ask what is the structure of ice critical nuclei for these models? Is it Ic or Ih? Since both polymorphs nucleate at the same speed, the critical nucleus will probably have a mixed cubic/hexagonal stacking. A random stacking would confer an extra disorder to the nucleus, both increasing its entropy[97] and making it kinetically more accessible. In fact, small clusters with mixed stacking have already been observed in simulations of the mW[15,25] and the TIP4P[26] models. In Refs. 23, 99, and 100, however, the structure of the mW ice growing from the liquid is reported to be predominantly cubic. The picture may be different in real water because the greater stability of ice Ih may lead to a preferred pathway via hexagonal clusters, specially at high temperatures.[97] In any case, what we want to stress with this work is that changing the structure of the critical clusters from ice Ih to ice Ic seeds does not affect the fair agreement between experimental nucleation rates and those of the TIP4P/Ice and TIP4P/2005 models calculated by the seeding technique.[19,20]

X. SUMMARY AND CONCLUSIONS

In this work, we use computer simulations to study two competing pathways in the nucleation of ice from supercooled water: one via an ice Ih critical cluster and another via an ice Ic critical cluster. We use both TIP4P/2005 and TIP4P/Ice water models to perform this research. To compute the nucleation

rate, we use the seeding technique, which combines classical nucleation theory with simulations of ice clusters embedded in the supercooled liquid. We obtain, within the uncertainty of our method, the same nucleation rate for both types of ice polymorphs. To compute the nucleation rate, we determine the various factors contributing to the classical nucleation theory expression for such quantity. One is the chemical potential difference between the solid and the fluid. To compute the chemical potential of the solid phases, we use the Einstein molecule variant of the Einstein crystal method and find that for both studied water models the chemical potential is the same. We also obtain the number of particles in the critical ice clusters as a function of the supercooling by performing simulations of ice clusters embedded in supercooled water at different temperatures. Both models predict that both ice polymorphs nucleate via clusters of the same size for a given value of the supercooling (temperature difference with respect to the melting temperature). Another factor contributing to the nucleation rate is the attachment rate, which gives an idea of the speed with which particles attach to the critical cluster. We measure the attachment rate by launching a few simulations of the critical cluster. Again, the attachment rate is the same for both ice polymorphs. Therefore, we conclude that the rate is the same for both ice I polymorphs because all factors contributing to it are the same within the uncertainty of our calculations. Our calculations of the size of the critical cluster combined with classical nucleation theory also allow us to estimate the ice-water interfacial free energy, which is the same for both ices, Ih and Ic.

Finally, we perform a study of the shape of the clusters. All results described in the previous paragraph have been obtained by assuming a spherical cluster shape. However, we consider the possibility that the cluster shape resembles that of the unit cell and study a cubic cluster of ice Ic embedded in supercooled water. We observe that the cluster's shape quickly transforms from cubic to spherical, confirming the validity of the hypothesis used throughout this work that the critical cluster is spherical.

ACKNOWLEDGMENTS

This work was funded by Grant No. FIS2013/43209-P of the MEC and by the Marie Curie Career Integration Grant No. 322326-COSAAC-FP7-PEOPLE-2012-CIG. C. Valeriani and E. Sanz acknowledge financial support from a Ramon y Cajal Fellowship. J. R. Espinosa acknowledges financial support from the FPI Grant No. BES-2014-067625. Calculations were carried out in the supercomputer facility Tirant from the Spanish Supercomputing Network (RES) (Project No. QCM-2015-1-0028).

APPENDIX: NUMBER OF PARTICLES IN THE CLUSTER

For the determination of the number of particles in the cluster, we use the rotationally invariant local-bond order parameter proposed in Ref. 101. Such order parameter is a scalar number, $\bar{q}_6$ in our case, that is computed for every particle and whose value depends on the positions of the selected particle and its neighbors within a certain range (3.5 Å). The way we calculate $\bar{q}_6$ is described in some detail in the Appendix of Ref. 102. A threshold value, $\bar{q}_{6,t}$, is used to discriminate between liquid-like and solid-like particles in the system. The nucleus is the largest cluster of solid-like particles present in the system. Liquid-like particles are those with $\bar{q}_6 < \bar{q}_{6,t}$ and solid ones those with $\bar{q}_6 > \bar{q}_{6,t}$. We choose the value of $\bar{q}_{6,t}$ that makes the fraction of particles wrongly labelled in the bulk solid and liquid phases the same. In Fig. 10(a), we plot the percentage of mislabelled particles for the liquid and for both ice I polymorphs as a function of $\bar{q}_{6,t}$ for the TIP4P/2005 model at 237 K. The liquid curve crosses each solid curve for a different value of $\bar{q}_{6,t}$. Therefore, according to our criterion, different thresholds are needed to distinguish the liquid from either solid. We use $\bar{q}_{6,t} = 0.358$ and $\bar{q}_{6,t} = 0.379$ to distinguish liquid-like from ice Ih and Ic-like particles, respectively. These thresholds have been calculated for a supercooling roughly in the middle of the range of studied supercooling. Therefore, we use the same thresholds for all supercoolings. We also use the same $\bar{q}_{6,t}$ s for both TIP4P/2005 and TIP4P/Ice. This is justified by comparing Figs. 10(a) and 10(b), where we show that the mislabelling curves for the TIP4P/Ice model cross at very similar values of $\bar{q}_{6,t}$ to those of the TIP4P/2005 model.

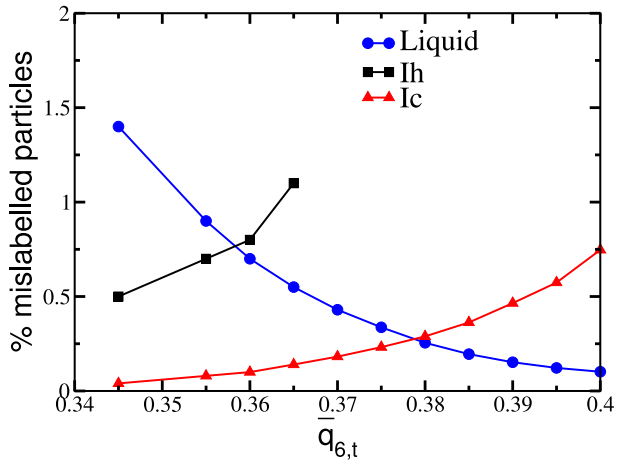

(a)

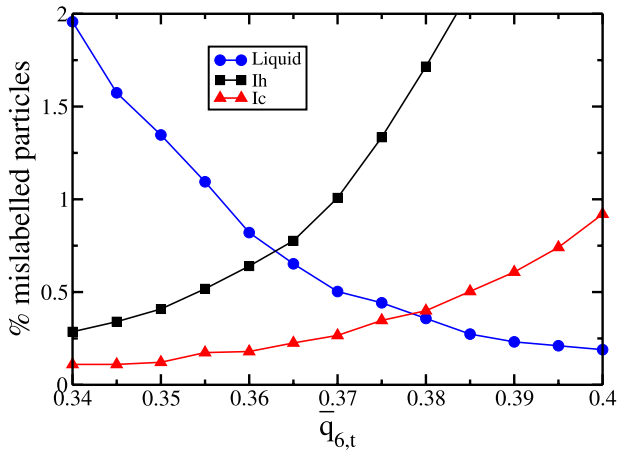

(b)

FIG. 10. Percentage of mislabelled particles in the bulk phase versus the selected threshold in the order parameter, $\bar{q}_{6,t}$. (a) and (b): Results for the TIP4P/2005 and TIP4P/Ice model at T = 237 K and T = 252 K, respectively.

[1]W. Cantrell and A. Heymsfield, Bull. Am. Meteorol. Soc. **86**, 795 (2005).
[2]M. B. Baker, Science **276**, 1072 (1997).
[3]P. J. DeMott, A. J. Prenni, X. Liu, S. M. Kreidenweis, M. D. Petters, C. H. Twohy, M. S. Richardson, T. Eidhammer, and D. C. Rogers, Proc. Natl. Acad. Sci. U. S. A. **107**, 11217 (2010).
[4]G. J. Morris and E. Acton, Cryobiology **66**, 85 (2013).
[5]S. S. Hirano and C. D. Upper, Microbiol. Mol. Biol. Rev. **64**, 624 (2000).
[6]L. R. Maki, E. L. Galyan, M.-M. Chang-Chien, and D. R. Caldwell, Appl. Microbiol. **28**, 456 (1974).
[7]J. K. Li and T. C. Lee, Trends Food Sci. Technol. **6**, 259 (1995).
[8]A. Michaelides and K. Morgenstern, Nat. Mater. **6**, 597 (2007).
[9]A. G. Gerrard, *Rocks and Landforms* (Springer, Netherlands, 1988).
[10]H. R. Pruppacher, J. Atmos. Sci. **52**, 1924 (1995).
[11]P. G. Debenedetti, *Metastable Liquids: Concepts and Principles* (Princeton University Press, 1996).
[12]P. Taborek, Phys. Rev. B **32**, 5902 (1985).
[13]D. A. Knopf and Y. J. Rigg, J. Phys. Chem. A **115**, 762 (2011).
[14]E. B. Moore and V. Molinero, Nature **479**, 506 (2011).
[15]T. Li, D. Donadio, G. Russo, and G. Galli, Phys. Chem. Chem. Phys. **13**, 19807 (2011).
[16]B. Riechers, F. Wittbracht, A. Hutten, and T. Koop, Phys. Chem. Chem. Phys. **15**, 5873 (2013).
[17]R. Radhakrishnan and B. L. Trout, Phys. Rev. Lett. **90**, 158301 (2003).
[18]I. M. Svishchev and P. G. Kusalik, Phys. Rev. Lett. **73**, 975 (1994).
[19]E. Sanz, C. Vega, J. R. Espinosa, R. Caballero-Bernal, J. L. F. Abascal, and C. Valeriani, J. Am. Chem. Soc. **135**, 15008 (2013).
[20]J. R. Espinosa, E. Sanz, C. Valeriani, and C. Vega, J. Chem. Phys. **141**, 18C529 (2014).
[21]M. Matsumoto, S. Saito, and I. Ohmine, Nature **416**, 409 (2002).
[22]D. Quigley and P. M. Rodger, J. Chem. Phys. **128**, 154518 (2008).
[23]A. Reinhardt and J. P. K. Doye, J. Chem. Phys. **136**, 054501 (2012).
[24]A. Reinhardt and J. P. K. Doye, J. Chem. Phys. **139**, 096102 (2013).
[25]E. B. Moore and V. Molinero, Phys. Chem. Chem. Phys. **13**, 20008 (2011).
[26]T. L. Malkin, B. J. Murray, A. V. Brukhno, J. Anwar, and C. G. Salzmann, Proc. Natl. Acad. Sci. U. S. A. **109**, 1041 (2012).
[27]P. Geiger and C. Dellago, J. Chem. Phys. **139**, 164105 (2013).
[28]F. Sciortino, I. Saika-Voivod, and P. H. Poole, Phys. Chem. Chem. Phys. **13**, 19759 (2011).
[29]S. J. Cox, S. M. Kathmann, B. Slater, and A. Michaelides, J. Chem. Phys. **142**, 184704 (2015).
[30]S. J. Cox, S. M. Kathmann, B. Slater, and A. Michaelides, J. Chem. Phys. **142**, 184705 (2015).
[31]G. Tammann, Ann. Phys. **2**, 1 (1900).
[32]W. Ostwald, Z. Phys. Chem. **22**, 289 (1897).
[33]H. Köning, Z. Kristallogr. **105**, 279 (1943).
[34]N. D. Lisgarten and M. Blackman, Nature **178**, 39 (1956).
[35]F. V. Shallcross and G. B. Carpenter, J. Chem. Phys. **26**, 782 (1957).
[36]L. G. Dowell and A. P. Rinfret, Nature **188**, 1144 (1960).
[37]J. E. Bertie and S. M. Jacobs, J. Chem. Phys. **67**, 2445 (1977).
[38]S. Klotz, J. M. Besson, G. Hamel, R. J. Nelmes, J. S. Loveday, and W. G. Marshall, Nature **398**, 681 (1999).
[39]D. D. Klug, Y. P. Handa, J. S. Tse, and E. Whalley, J. Chem. Phys. **90**, 2390 (1989).
[40]W. F. Kuhs, C. Sippel, A. Falenty, and T. C. Hansen, Proc. Natl. Acad. Sci. U. S. A. **109**, 21259 (2012).
[41]B. J. Murray, S. L. Broadley, T. W. Wilson, S. J. Bull, R. H. Wills, H. K. Christenson, and E. J. Murray, Phys. Chem. Chem. Phys. **12**, 10380 (2010).
[42]T. L. Malkin, B. J. Murray, C. G. Salzmann, V. Molinero, S. J. Pickering, and T. F. Whale, Phys. Chem. Chem. Phys. **17**, 60 (2015).
[43]D. Rozmanov and P. G. Kusalik, Phys. Chem. Chem. Phys. **13**, 15501 (2011).
[44]M. A. Carignano, J. Phys. Chem. C **111**, 501 (2007).
[45]B. J. Murray, D. A. Knopf, and A. K. Bertram, Nature **434**, 202 (2005).
[46]E. Mayer and A. Hallbrucker, Nature **325**, 601 (1987).
[47]T. C. Hansen, M. M. Roza, P. Lindner, and W. F. Kuhs, J. Phys.: Condens. Matter **20**, 285105 (2008).
[48]I. Kohl, E. Mayer, and A. Hallbrucker, Phys. Chem. Chem. Phys. **2**, 1579 (2000).
[49]B. J. Murray and A. K. Bertram, Phys. Chem. Chem. Phys. **8**, 186 (2009).
[50]P. Jenniskens, S. F. Banham, D. F. Blake, and M. R. S. McCoustra, J. Chem. Phys. **107**, 1232 (1997).
[51]D. Murphy, Geophys. Res. Lett. **30**, 2230, doi:10.1029/2003GL018566 (2003).
[52]Y. P. Handa, D. D. Klug, and E. Whalley, Can. J. Chem. **66**, 919 (1988).
[53]O. Yamamuro, M. Oguni, T. Matsuo, and H. Suga, J. Phys. Chem. Solids **48**, 935 (1987).
[54]J. A. McMillan and S. C. Los, Nature **206**, 806 (1965).
[55]J. Shilling, M. Tolbert, O. Toon, E. Jensen, B. Murray, and A. Bertram, Geophys. Res. Lett. **33**, L17801, doi:10.1029/2006GL026671 (2006).
[56]X. M. Bai and M. Li, J. Chem. Phys. **124**, 124707 (2006).
[57]C. Vega and E. G. Noya, J. Chem. Phys. **127**, 154113 (2007).
[58]D. Frenkel and A. J. C. Ladd, J. Chem. Phys. **81**, 3188 (1984).
[59]J. L. F. Abascal and C. Vega, J. Chem. Phys. **123**, 234505 (2005).
[60]J. L. F. Abascal, E. Sanz, R. G. Fernandez, and C. Vega, J. Chem. Phys. **122**, 234511 (2005).
[61]J. Benet, L. G. MacDowell, and E. Sanz, Phys. Chem. Chem. Phys. **16**, 22159 (2014).
[62]C. Vega, M. Martin-Conde, and A. Patrykiejew, Mol. Phys. **104**, 3583 (2006).
[63]C. Vega and J. L. F. Abascal, Phys. Chem. Chem. Phys. **13**, 19663 (2011).
[64]H. J. C. Berendsen, J. R. Grigera, and T. P. Straatsma, J. Phys. Chem. **91**, 6269 (1987).
[65]M. W. Mahoney and W. L. Jorgensen, J. Chem. Phys. **112**, 8910 (2000).
[66]W. L. Jorgensen, J. Chandrasekhar, J. D. Madura, R. W. Impey, and M. L. Klein, J. Chem. Phys. **79**, 926 (1983).
[67]E. Sanz, C. Vega, J. L. F. Abascal, and L. G. MacDowell, Phys. Rev. Lett. **92**, 255701 (2004).
[68]M. M. Conde, M. A. Gonzalez, J. L. F. Abascal, and C. Vega, J. Chem. Phys. **139**, 154505 (2013).
[69]X. M. Bai and M. Li, J. Chem. Phys. **123**, 151102 (2005).
[70]B. C. Knott, V. Molinero, M. F. Doherty, and B. Peters, J. Am. Chem. Soc. **134**, 19544 (2012).
[71]V. Jacobson and L. C. Molinero, J. Am. Chem. Soc. **133**, 6458 (2011).
[72]J. R. Espinosa, C. Vega, C. Valeriani, and E. Sanz, J. Chem. Phys. **142**, 194709 (2015).
[73]K. F. Kelton, *Crystal Nucleation in Liquids and Glasses* (Academic, Boston, 1991).
[74]R. Becker and W. Doring, Ann. Phys. **24**, 719 (1935).
[75]M. Volmer and A. Weber, Z. Phys. Chem. **119**, 277 (1926).
[76]S. Auer and D. Frenkel, J. Chem. Phys. **120**, 3015 (2004).
[77]S. Auer and D. Frenkel, Nature **409**, 1020 (2001).
[78]C. Vega, E. Sanz, J. L. F. Abascal, and E. Noya, J. Phys.: Condens. Matter **20**, 153101 (2008).
[79]E. G. Noya, M. M. Conde, and C. Vega, J. Chem. Phys. **129**, 104704 (2008).
[80]M. P. Allen and D. J. Tildesley, *Computer Simulation of Liquids* (Oxford University Press, 1987).
[81]D. Frenkel and B. Smit, *Understanding Molecular Simulation* (Academic Press, London, 1996).
[82]M. Parrinello and A. Rahman, J. Appl. Phys. **52**, 7182 (1981).
[83]S. Yashonath and C. N. R. Rao, Mol. Phys. **54**, 245 (1985).
[84]V. Buch, P. Sandler, and J. Sadlej, J. Phys. Chem. B **102**, 8641 (1998).
[85]E. A. Engel, B. Monserrat, and R. J. Needs, Phys. Rev. X **5**, 021033 (2015).
[86]J. M. Polson, E. Trizac, S. Pronk, and D. Frenkel, J. Chem. Phys. **112**, 5339 (2000).
[87]J. R. Espinosa, E. Sanz, C. Valeriani, and C. Vega, J. Chem. Phys. **139**, 144502 (2013).
[88]C. Vega, J. L. F. Abascal, M. M. Conde, and J. L. Aragones, Faraday Discuss. **141**, 251 (2009).
[89]J. L. F. Abascal and C. Vega, J. Phys. Chem. C **111**, 15811 (2007).
[90]E. Lindahl, B. Hess, and D. van der Spoel, J. Mol. Model. **7**, 306 (2001).
[91]D. Rozmanov and P. G. Kusalik, Phys. Chem. Chem. Phys. **14**, 13010 (2012).
[92]L. Ickes, A. Welti, C. Hoose, and U. Lohmann, Phys. Chem. Chem. Phys. **17**, 5514 (2015).
[93]R. L. Davidchack, R. Handel, J. Anwar, and A. V. Brukhno, J. Chem. Theory Comput. **8**, 2383 (2012).
[94]C. Valeriani, E. Sanz, and D. Frenkel, J. Chem. Phys. **122**, 194501 (2005).
[95]F. Smallenburg, P. H. Poole, and F. Sciortino, Mol. Phys. (published online 18 May 2015).
[96]V. Molinero and E. B. Moore, J. Phys. Chem. B **113**, 4008 (2009).
[97]D. Quigley, J. Chem. Phys. **141**, 121101 (2014).
[98]J. Russo, F. Romano, and H. Tanaka, Nat. Mater. **13**, 733 (2014).
[99]A. Haji-Akbari and P. G. Debenedetti, Proc. Natl. Acad. Sci. U. S. A. **112**, 10582 (2015).
[100]C. Buhariwalla, R. Bowles, I. Saika-Voivod, F. Sciortino, and P. Poole, Eur. Phys. J. E **38**, 39 (2015).
[101]W. Lechner and C. Dellago, J. Chem. Phys. **129**, 114707 (2008).
[102]J. Benet, L. G. MacDowell, and E. Sanz, J. Chem. Phys. **141**, 024307 (2014).